Computer modeling of bevacizumab drug distribution after intravitreal injection in rabbit and human eyes

Jabia M. Chowdhury[1], Katelyn E. Swindle-Reilly[2,3], and Ashlee N. Ford Versypt[1,4,5,*]

[1]Department of Chemical and Biological Engineering, University at Buffalo, The State University of New York, Buffalo, NY, USA
[2]William G. Lowrie Department of Chemical and Biomolecular Engineering, The Ohio State University, Columbus, OH, USA
[3]Department of Biomedical Engineering, The Ohio State University, Columbus, OH, USA
[4]Department of Biomedical Engineering, University at Buffalo, The State University of New York, Buffalo, NY, USA
[5]Institute for Artificial Intelligence and Data Science, University at Buffalo, The State University of New York, Buffalo, NY, USA
[*]Corresponding author: Ashlee N. Ford Versypt, ashleefv@buffalo.edu

May 4, 2023

Abstract

Macula clears our central vision and sharpens our visibility. The macula is positioned in the middle of the retinal tissue. Age-related macular degeneration (AMD) is a condition brought on by macular deterioration. In the United States, millions of elderly people suffer from AMD. There is no permanent cure if the disease is diagnosed at a later stage. AMD is an irreversible disease where the patient goes blind eternally. For retinal treatment, due to the material characteristics of the vitreous humor layer, it serves as the main barrier to drug transport to the retinal layer. Many treatments, including drug-based treatment, laser photocoagulation, and laser therapy, have been used for AMD disease. Anti-VEGF drugs have been proven most stable medication in AMD treatment that inhibits the action of vascular endothelial growth factor. One of the most suggested anti-VEGF drugs used in AMD treatment is bevacizumab using intravitreal injection. In our study, we have developed a spatially distributed pharmacokinetic model of the drug bevacizumab to measure time-drug concentration profiles throughout the vitreous and near the macula in rabbit and human eyes.

1 Introduction

Retinal neovascular diseases are considered the most common cause of vision loss in all age groups. The retina is located at the back of the eye, and it consists of several layers of cells including the macula. The macula is positioned at the center of the retina and it is responsible for clarity of vision. Hypoxia happens when a cell receives less oxygen than required and this condition causes vascular

endothelial cell growth. It promotes aberrant blood vessels in the macula and causes the irremediable disease called age-related macular degeneration (AMD). AMD damages the macula and affects the center of the visual field, which limits the patient's ability to see or recognize any object.

In the United States, there are around 11 million people who have suffered from AMD [1, 2]. AMD is generally found in aged people, older than 65 years [3, 4]. AMD is considered an irreversible disease that causes vision loss when it is identified at advanced stages. Early detection of AMD disease could reduce the visual impairment of the patient. There are two types of AMD: non-neovascular (dry) AMD and neovascular (wet) AMD.

The vitreous humor(VH) has viscoelastic properties and fills with a colorless, transparent, gel-like material that contains 99% of water [5, 6]. The vitreous humor(VH) is located at the center of the eye, between the lens and the retina and it covers 80% volume of the eye [7]. VH maintains the shape and size of the eye and protects the retina from any disturbing substances as VH is rigidly attached to certain areas of the retina. Treatment of inner retinal diseases is challenging because of the anatomical complexity of the posterior segment of the eye. The vitreous is surrounded by the hyaloid membrane and it is exceedingly difficult to penetrate any substance through the vitreous to the retinal layer due to its resistant properties.

Vascular endothelial growth factor (VEGF) is a type of protein that is essential in the growth of blood vessels. VEGF is in charge of signaling molecules to promote new blood vessel production while facing a condition of hypoxia. The overproduction of protein causes the disordered growth of new blood vessels in the retinal layer like the macula. Though VEGF is beneficial in other parts of the body such as the heart muscle, it is harmful to the eye. Overproduction of VEGF in the macula causes the retinal neovascular disease called AMD. Anti-VEGF drugs are the key mediator and are widely accepted to treat retinal neovascular diseases like AMD. There are five most commonly used anti-VEGF drugs used in AMD treatment, approved by US Food and Drug Administration (FDA) [8]. In this work, one of the most used anti-VEGF drugs, bevacizumab (Avastin), is used in our computational drug delivery model to investigate the pharmacokinetic behavior.

Different ocular therapeutic approaches, like intravitreal injection, drug implant, laser photocoagulation, and photodynamic therapy, are effective in retinal diseases like AMD. It has also been found in research that high-dose vitamin supplementation is recommended to reduce vision loss in AMD treatment [9]. Intravitreal injection of anti-VEGF drug administration is considered the most popular option in AMD treatment [10]. Intravitreal injection allows high drug concentration to the retinal layer with minimal side effects in ocular treatment. In our current work, we used the drug bevacizumab by intravitreal injection to observe the pharmacokinetic aspects in the vitreous and near macula. The drug release from intravitreal injection using the drug diffusion coefficient of bevacizumab in rabbit vitreous was not taken into account in any known computational research.

Several experiments have been done to investigate the pharmacokinetic effect of the drug bevacizumab in animals and observe the time-concentration plot [11, 12, 13]. There has not been much work done on developing a computational drug delivery model using bevacizumab. One research study has been found to analyze *in silico* model of bevacizumab release from intravitreal drug-loaded PLGA microspheres and observe the drug distribution profile [14]. The weakness of this work is, the drug diffusion coefficient used in the simulation and taken from [15] was not for the drug bevacizumab, but the drug triamcinolone acetonide (TA) [15]. The molecular weight (MW) of the drug bevacizumab is 149 kDa and drug TA has an MW of 434.5 g/mol (0.434 kDa). Since bevacizumab is a much heavier drug than TA, the value of the drug diffusion coefficient for these two drugs is not close enough to use in the simulation purpose. This work includes bevacizumab release from intravitreal administrated PLGA microspheres whereas, in our model, we consider intravitreal injection.

Hutton-Smith [16] published a mechanistic model of intravitreal pharmacokinetics and pharmacodynamic aspects of using ranibizumab drug used in AMD treatment. The goal of our current work is not similar to their research goal, as their major focus was to capture the response of the drug reducing the ocular vascular endothelial growth factor in patients besides the pharmacokinetic (PK)

effect. Their PK studies focused on calculating ocular half life for various drugs in animal species data. Whereas in our work, we observe the pharmacokinetic effect of the drug and measure the drug bevacizumab concentration near the macula region and observe the duration of the required amount of drug present at that location. To our knowledge, our model is the first known computational model to study the pharmacokinetic effect of intravitreally injected drug bevacizumab in both human and rabbit eyes and calculate the time-concentration plot near the macula region.

In AMD treatment, the target of the drug is to control the abnormal cell/blood vessel growth in the macula. The most frequent treatment used in AMD is intravitreal injections. Drug transport to the retinal layer depends on the anatomical properties of the vitreous in the eye. Different investigations have been done to simulate the vitreous humor region. Khoobyar et al. [17] considered the vitreous humor as a porous media and divided the porous region as gel and liquefied region described by the Darcy flow. This aspect of these methods needs more investigation. Balachandran [18] considered the vitreous motion and mode of vitreous humor using a saccade-induced flow field. Researchers noticed that the degree of liquefaction was correlated with an increase in vitreous mobility, which is caused by fast ocular oscillations. Ocular oscillations, also known as saccades, assist in orienting the line of sight and enable us to regularly concentrate at various locations. Rapid saccades may cause the vitreous to swirl at high speeds, leading to considerable convective transfer. These methods faced difficulties and challenges while solving numerically and provide complexity while solving fluid flow in the vitreous. Brinkman's equation is another way to solve the porous media, and it was used by [19] while solving the computational analysis of vitreous humor and used Darcy's law analytically to solve their model. Vitreous humor is a gel-like porous structure, and the fluid that transports through the vitreous is described with accuracy by using Darcy's law. The researcher used mostly Darcy's law and then Brinkman's equation to implement the vitreous humor.

In this work, we developed a time-dependent, three-dimensional model for intravitreal drug delivery in the posterior segment of the eye, specifically in the retinal layer. We used the recombinant humanized monoclonal antibody drug bevacizumab. Our target of using this injected anti-VEGF agent into the vitreous humor is to observe the drug concentration in the target location, near the macula. We studied the pharmacokinetic effect of the drug and validated the time-concentration plot in the vitreous with the experimental PK results taken from rabbit eyes and human eyes. We also investigated drug transport by changing the location of drug administration and observed the spatial distribution of the drug in the vitreous humor. In our model, we calculated the time-concentration plot near the macula region in both rabbit and human eyes to determine the maximum duration of the required drug amount that remained near the macula region after intravitreal injection.

2 Methods

The pharmacokinetics study is used to evaluate the time course of medications and their effects on the body and explains the processes of absorption, distribution, metabolism, and excretion (ADME). Although a computational pharmacokinetic model utilizing the anti-VEGF medication bevacizumab has seen very little research, an experimental PK model using rabbit eyes is available. Our computational PK study takes both the pharmacokinetic analyses of anterior and posterior elimination into account when analyzing the distribution and absorption of the intravitreally injected drug bevacizumab. Our computational PK does not include the effect of metabolism and degradation, as the metabolism and degradation of anti-VEGF agents in the eye are negligible [20].

COMSOL Multiphysics is a commercial finite element software that has a built-in "physics interface" environment. In this work, two major physics interfaces are used in COMSOL. Darcy's law is used to simulate vitreous humor as a porous structure and "mass and species transport" physics is used to transport the drug through the vitreous in the 3D geometric model. Darcy's law is coupled with the mass transport physics by Darcy's velocity field while defining the transport properties of the

vitreous. The simulation was done in COMSOL 6.1 under time-dependent conditions.

2.1 Geometry

We have created a three-dimensional geometry of the vitreous humor for rabbit and human eyes. The shape of vitreous humor is considered spherical in our model. The major difference between a rabbit and human vitreous humor is the size. In the rabbit eye, the size of the lens is the same as the vitreous humor, which is around 6.2 mm. The large size of the lens reduces the size of the vitreous in rabbits. The human vitreous is approximately three times bigger than the rabbit vitreous. The volume of the vitreous in rabbit eye varies from 1.4 mL to 1.7 mL [21]. The dimension of human and rabbit vitreous used in our model were taken from another study by Missel [22]. The geometrical shapes of both our models are influenced by the geometry from Khoobyar et al. [17]. Human vitreous is larger in shape and its volume range varies between 4.1 and 4.4 mL [23]. We found a larger dimension of human vitreous reported in Missel's model, which is between 4.7 and 4.8 mL [22]. We fixed our geometry of the human vitreous as 4.9 mL and the rabbit vitreous as 1.4 mL. The other three major tissues–retina, lens, and hyaloid membrane–are bounded around the vitreous humor, which is considered in our geometry and is shown in Fig. 1a. Fig. 1 shows the geometrical model where (a) and (b) shows the 3D plot of the vitreous in the human eye, explaining the outer layers and boundary conditions, (c) shows the 2D plot of the human eye, (d) shows the 2D plot of the rabbit eye. We have created our geometry in COMSOL 6.1.

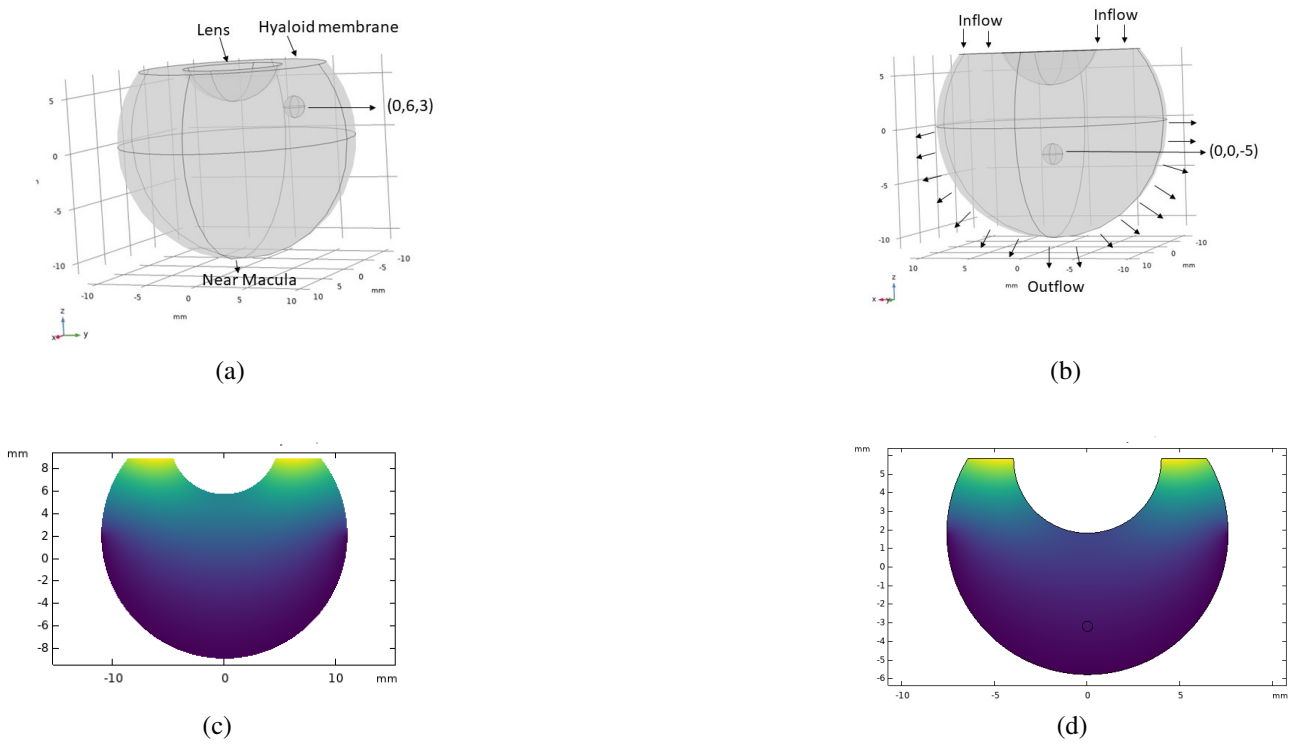

Figure 1: Geometry of our ocular model (a) 3D geometry of human vitreous shows major tissues of our model (b) 3D geometry of human vitreous showing the boundary condition (c) 2D plot of human vitreous (d) 2D plot of rabbit vitreous

2.2 Fluid dynamics modeling of vitreous humor

Vitreous humor is treated as a porous structure due to its viscoelastic properties. The healthy young vitreous is an intact viscoelastic gel-like material and it gets to liquefy with age [7]. We considered the vitreous to be stationary, incompressible, and porous with high porosity since collagen fibers were present in it. Additionally, we regarded all layers as porous media, and the fluid velocity in the VH is assumed to be very low [24]. The aqueous humor permeates the vitreous and posterior layers through the hyaloid membrane, resulting in the convective mass movement. Previous studies used different approaches to solve the vitreous humor simulation in computational drug delivery models. Brinkman's equation and Darcy's law are two common methods used to simulate the vitreous humor as a porous structure. In this study, we are using Darcy's law to solve the vitreous humor as a porous media influenced by [17].

The governing equation used in Darcy's law is given by

$$\vartheta = \left(\frac{\kappa}{\mu}\right)\nabla p \tag{1}$$

$$\frac{\partial}{\partial t}(\rho\varepsilon) + \nabla\cdot(\rho\vartheta) = Q_m \tag{2}$$

where κ is the permeability, ρ is the density, ε is the porosity, μ is the dynamic viscosity, ϑ is Darcy's velocity, p is the fluid pressure, and Q_m is the mass source term and. In COMSOL these parameters are used to define the vitreous material properties.

2.3 Drug transport modeling in the vitreous humor

Treatment of inner retinal diseases is challenging for ocular anatomical barriers. Four routes are commonly used in ocular drug delivery in the posterior segment of the eye [25]. Drug transport in the vitreous is not linearly distributed and fully understood. The dependent factors for drug distribution in the vitreous are human anatomy, the shape of the eye, vitreous properties, and the ocular topography of individuals. We administrated the drug bevacizumab using an injection in the vitreous humor in two different locations and observed drug concentration at the targeted tissue. In our study, the PK model captures the continuum of drug movement through the vitreous tissues by diffusion and convection by the aqueous humor fluid passing in the vitreous. As it was previously mentioned, the target of the drug bevacizumab is the near macula region, located in the middle of the retina and attached to the outer boundary of the vitreous.

Diffusive transport of the drug bevacizumab from intravitreal injection in the vitreous humor and convective transport of the drug due to aqueous humor fluid flow in the vitreous as an inlet fluid velocity were modeled as transport of diluted species in porous media. Drug kinetics is governed by both diffusive transport due to concentration gradient ∇c and by convective transport due to AH flow with velocity u. The governing equation of drug molecule transport in the vitreous humor is

$$\frac{\partial C}{\partial t} + \nabla\cdot -(D\nabla c) + u\cdot\nabla c = R \tag{3}$$

where C is the drug concentration, u is the flow velocity, the term $u\cdot\nabla c$ represents the mass transport due to convection, D represents the diffusion coefficient of the drug, and R represents the reaction rate, which is zero in our model. The term $-D\nabla c$ describes how much the drug bevacizumab diffuses through the vitreous.

2.4 Model parameters and boundary conditions

In our study, we created 3D spherical geometry of the vitreous humor surrounded by the hyaloid membrane, lens, and outer surface of the vitreous which is attached to the retinal layer. Fig. 1 includes the 3D and 2D geometric plots of human and rabbit eyes used in our model. The hyaloid membrane is a highly porous thin membrane that separates the vitreous from the anterior segment of the eye. Drug transport was modeled using a convection-diffusion equation coupled with the velocity profile obtained from Darcy's law in the porous domain. The effect of drug diffusion in the vitreous and convection caused by the constant permeation of aqueous humor through the vitreous is considered. Fig. 2 includes the 3D figure of the geometric model that summarizes all of the boundary conditions.

VH material parameters are defined using the hydraulic conductivity $(\frac{\kappa}{\mu})$ of rabbit vitreous, which is 5.8×10^{-15} m^2/Pa.s [20], and human vitreous, which is 9×10^{-7} mm^2/Pa.s [17]. The aqueous humor fluid produces from the ciliary body and enters the vitreous cavity through the retrozonular and retrolental spaces and we assumed that aqueous humor fluid moves through the vitreous humor [26]. The aqueous humor permeates the vitreous through the hyaloid membrane and we considered it as an inlet fluid velocity in our model (Fig. fig:3DgeomwBC). The fluid pressure is maximum in the outflow pathway of the trabecular meshwork and episcleral venous which are not part of our geometry. The pressure in the vitreous is considered to be zero, which is set as an outflow boundary condition (Fig. fig:3DgeomwBC). We have applied a no-flux boundary condition at the lens surface as it is impermeable to water and drugs. The no-flux boundary condition is defined by

$$-\mathbf{n} \cdot \rho u = 0 \tag{4}$$

where $\mathbf{n}$ is the unit normal vector.

The initial condition in Darcy's law is set as zero for all boundaries is defined by

$$p = 0 \tag{5}$$

Table 1 includes all the parameters used to define Darcy's law.

Table 1: Parameter values for Darcy's law

Description	Human	Rabbit	Unit	Reference
Density	1008	1008	kg/m^3	[27]
Viscosity	0.1	0.1	Pa·s	[17], [20]
Permeability	9×10^{-7}	5.8×10^{-9}	mm^2	[17],[20]
Inlet	0.00015	0.00015	mm/s	[17]
Outlet	0	0	Pa	[17]

The drug transport through the virtuous is solved using transport of diluted species physics in COMSOL. The lower level dose concentration for bevacizumab administration is 1.25mg/0.05mL [28, 11, 29], and this concentration will be used for both humans and rabbits. The target location of the drug bevacizumab is the macula, and our PK studies measured the drug concentration near the macula region. The drug release rate depends on the drug diffusion coefficient value. The diffusion coefficient of the drug bevacizumab in rabbit vitreous humor is $1.2 \pm .6 \times 10^{-6}$ cm^2/s [30]; for human vitreous humor, we used the value of diffusion coefficient as 9.13×10^{-7} cm^2/s [16].

The vitreous is located in the 3D domain with its origin at $(x,y,z) = (0,0,0)$ and a radius of 11 mm for human vitreous and 7.6 mm radius for rabbit vitreous. The injection shape is considered to be a sphere with a 0.3 mm radius. The injected location is centered at the (0,6,4) coordinate or at (0,0,-5) for some cases. The concentration at the injected location is defined as C_i ,and the value of

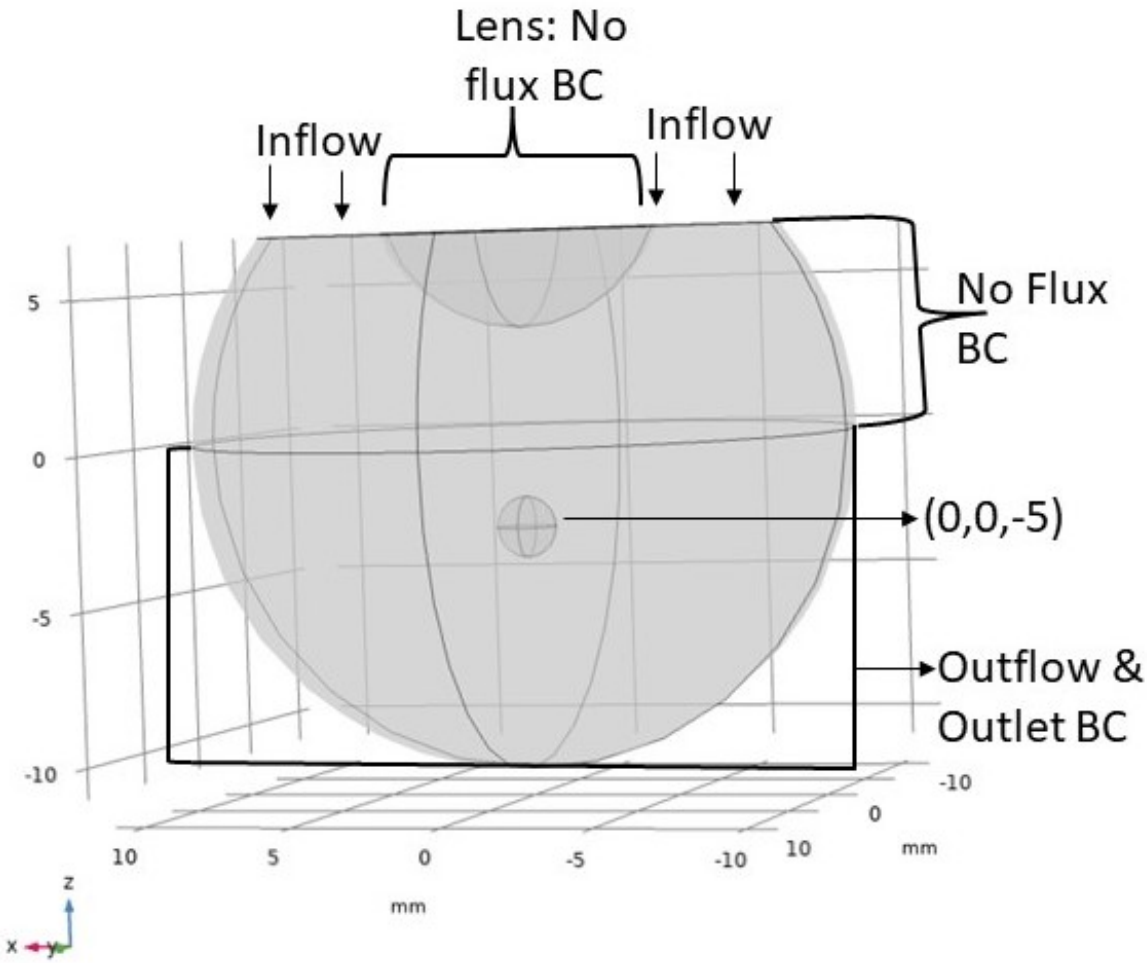

Figure 2: 3D geometry with boundary conditions

the injected drug concentration is $C_i = 0.167$ mol/m^3. The initial drug concentration C_0 in the domain is defined as

$$C_0 = \begin{cases} C_i & \text{for } (x-0)^2 + (y-6)^2 + (z-4)^2 = (0.3)^2 \\ 0 & \text{otherwise} \end{cases} \tag{6}$$

The major routes of drug elimination are through the aqueous humor drainage and blood-retinal barrier [20]. We considered the hyaloid membrane surface and the outer surface of the vitreous humor as the anterior and posterior routes for drug elimination, respectively. The drug outflow boundary condition is defined by

$$n \cdot D\nabla c = 0 \tag{7}$$

3 Results and discussion

Our investigation does not find any other available data except [14] on the computational PK model using bevacizumab. Experimental data are available for both human and rabbit eyes to validate our PK data of the time-concentration plot in the vitreous. Heljak and Swieszkowski [14] published an *in silico* model and claimed to use the drug bevacizumab; however, the reference data shows using properties for the drug triamcinolone acetonide. Because of the property differences between triamcinolone acetonide and bevacizumab, we did not consider their results in our model. To validate our computational model we considered the experimental results of pharmacokinetic studies using WebPlotDigitizer [31] software to collect the data of the drug bevacizumab concentration in vitreous humor in rabbit and human eyes. We have not found any experimental data that calculates drug concentration in the macula or near the macula region. The experimental data do not contain each time point up to 65 days, so we observe the discrepancy in the results section not having as many values as our computational model has.

3.1 Rabbit eye

There is currently no cure for AMD, however, due to its nature of action, a significantly lower dose of bevacizumab drug (1.25mg/0.05mL) is used. The drug bevacizumab is injected intravitreally behind the surgical limbus using a 30-gauge needle [11], which is the most common injected position applying most of the experimental studies. To measure the drug concentration of the vitreous in experimental studies, the vitreous was withdrawn from enucleated rabbit eye using a 30-gauge needle. The experimental results showed PK studies were performed not only in vitreous but also in aqueous and serum of rabbit eye following the same procedure [11, 13, 32]. Other pharmacokinetic studies investigate drug concentration in the iris and ciliary body and retina and choroid tissue.

In our 3D model, we measured the concentration of the drug bevacizumab in the vitreous and near macula region. In our geometry, as we did not include the retinal layer, we fixed the point shown in Fig. 1(a) to measure the drug concentration at the bottom of the outer vitreous and defined this area as the near macula region. We have collected data from previously performed experimental results from the rabbit eye model to validate our study. The experimental PK analysis generated time-concentration plots using compartmental methods. We observed from different pharmacokinetic experiments, the drug bevacizumab concentration in VH varied after the first day of intravitreal administration, as we found from [11], the drug concentration in VH was 925.69 μg/mL [11], where other experiments found 109.81 μg/mL [33] and 159.2 μg/mL [32]. These data were collected from prior publications using WebPlotDigitizer [31].

Fig. 3 shows the drug concentration-time plot in rabbit vitreous, taken from experimental studies to validate our computational model [11, 28, 34]. These experiments were done following a similar methodology, briefly, 1.25 mg/0.05 mL of bevacizumab was injected near the limbus region in rabbit vitreous using 30-gauge needles. Fig. 3 shows the maximum concentration C_{max} value is 925.69

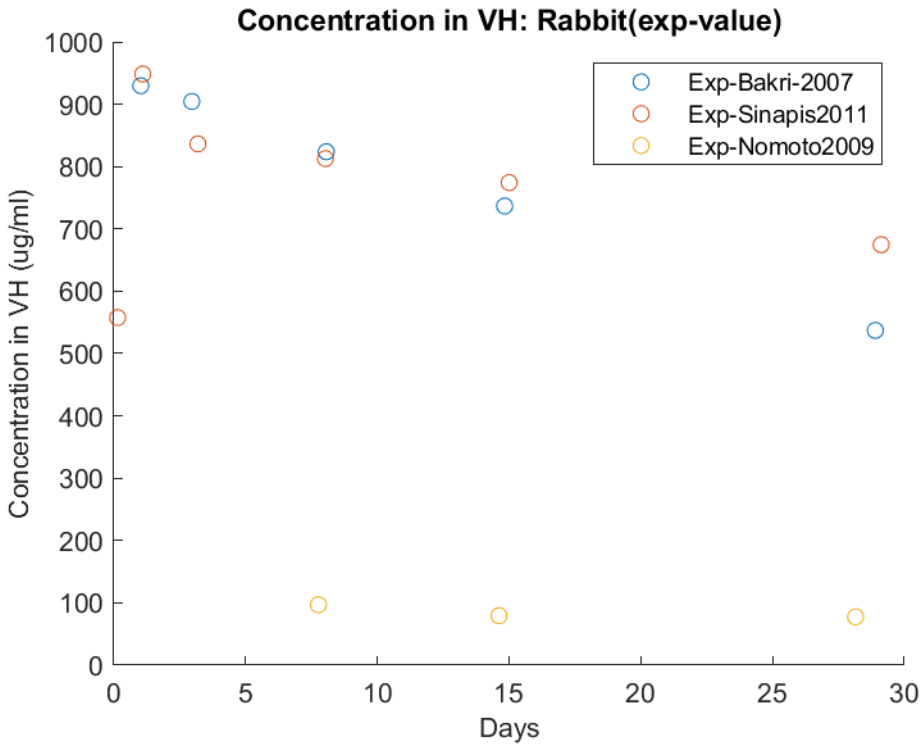

Figure 3: VH concentration in rabbit eye: experimental results

μg/mL from [11] whereas [28] had a 948.48 μg/mL maximum value, and from [34] the C_{max} value was 97.04 μg/mL. Many pharmacokinetic studies measured the time-concentration plot in rabbits but the reason for including these three PK studies in our work is that the methodology of experimenting with rabbits are same. The drug transport mechanism in the vitreous humor is not completely understood and it depends on several factors like anatomy, shape, vitreous properties, and another factor of the eye. For this reason, despite following the same methods, the drug concentration is not followed the same pattern for those experimental studies included in Fig. 3.

Using injection for drug administration is the process where the drug starts diffusing so fast and the drug release rate is very high. Other drug administration processes like using nanoparticles and PLGA microspheres can slow the drug release rate. In our computational model, we have found the maximum concentration is 10.01 μg/mL. In Fig. 4, bevacizumab time-concentration profiles in the vitreous after the intravitreal injection are presented for results from our computational simulations and the experimental results presented in Fig. 3. We observed that drug transport is very fast in [34] when compared to the other two experimental studies. But in our computational model, it transports faster than those experimental studies.

Our pharmacokinetic studies included the drug bevacizumab concentration near the macula region. In AMD treatment, the purpose of using anti-VEGF drugs is to control the cell growth in the macula and the target location of drug bevacizumab is the macula. We have not found any experimental data available measuring drug concentration near the macula in human and rabbit eyes. To control the endothelial cell growth to inhibit VEGF completely, the minimum concentration of the drug bevacizumab needs to be 500 ng/mL [33]. In our computational model, the maximum concentration (C_{max}) near the macula is 10.06 μg/mL while injecting in the central vitreous and near the limbus location. Our studies investigated the pharmacokinetic effect of the drugs in two different positions influenced by [17] and [35]. Friedrich et al. [35] highlighted that the drug injected position affects drug distribution and elimination in vitreous and pointed to four injected positions as a) central injection b) injected next to the symmetry axis c) next to the retina on the symmetry axis and d) close to the hyaloid membrane. Khoobyar et al. [17] included a 2D plot of the drug distribution in different positions after intravitreal injection and showed the spatial drug distribution profile in the

human eye. However, we fixed the drug injected location near the limbus (0,6,3), and the other one is fixed in the middle of the vitreous (0,0,-5) for administrating 1.25 mg/0.05mL drug bevacizumab. The drug-injected location is added in Fig. 1(a).

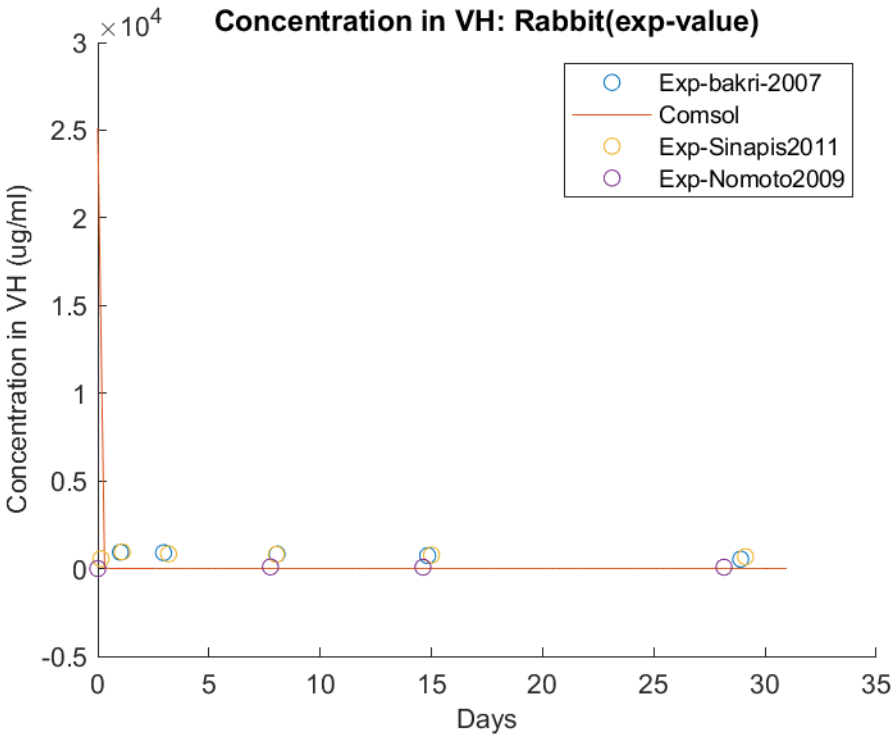

Figure 4: VH concentration plot in rabbit eye: experimental and computational

Fig. 5 shows the time-concentration plot of the drug bevacizumab near the macula for two different positions. Changing the location of drug administration can maximize the concentration C_{max} near the macula region. When the drug is administered in the central vitreous, this location is closer to the macula region and we observed the drug reached the macula very fast and the drug concentration reaches higher as 3.031 µg/mL. The C_{max} value is 0.2 µg/mL when injected near the lower limbus location than the drug administrated at the central vitreous. The major purpose of using this drug is to reduce the VEGF growth and for this, the minimum concentration of the drug bevacizumab is 500 ng/mL to control the cell growth in the macula. In our model, we observed the drug concentration goes lower than 500 ng/mL after 5.5 days when the drug was injected in the central vitreous(0,0,-5). The most interesting finding of our model is, the drug concentration remains more than 500 ng/mL for up to 70 days while injected near the limbus region(0,6,3). It means the required amount of drug present near the macula region to treat AMD is up to 70 days while injected in the limbus region which is the maximum amount of days compared to injected in the central vitreous location.

Fig. 6 shows the spatial distribution of drug transport after injected drug bevacizumab in central the vitreous region (0,0,-5) for three different time points in a 2D plot. Fig. 7 shows the drug transport in 3D geometry after the drug is injected near the limbus region.

3.2 Human eye

We found few available data on measuring drug bevacizumab concentration on the human vitreous. We followed the same methods, and boundary conditions to simulate the human model in 3D human geometry. The drug diffusion coefficient of the human eye is used as 9.13×10^{-7} cm^2/s [16]. This value is mathematically calculated so we checked the drug diffusion coefficient of other drugs in human use in AMD disease and found that the magnitude is the same as the rabbit value, which motivates

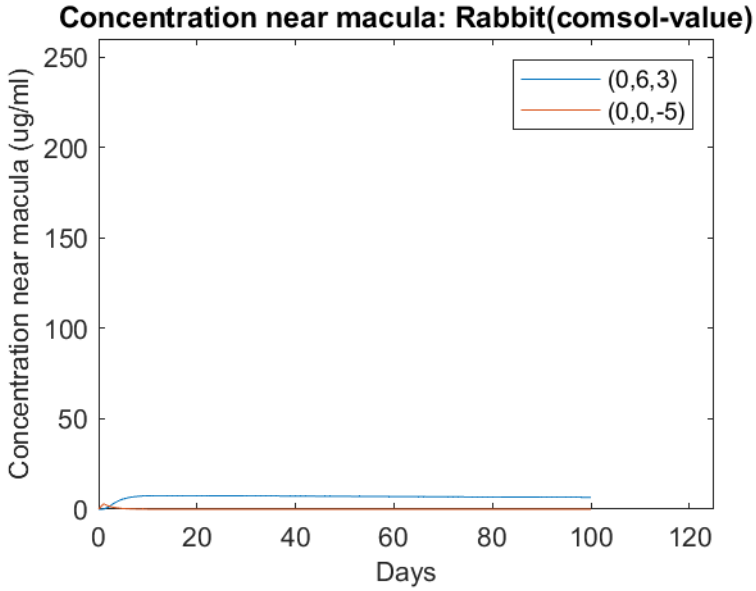

Figure 5: Drug concentration near macula: rabbit

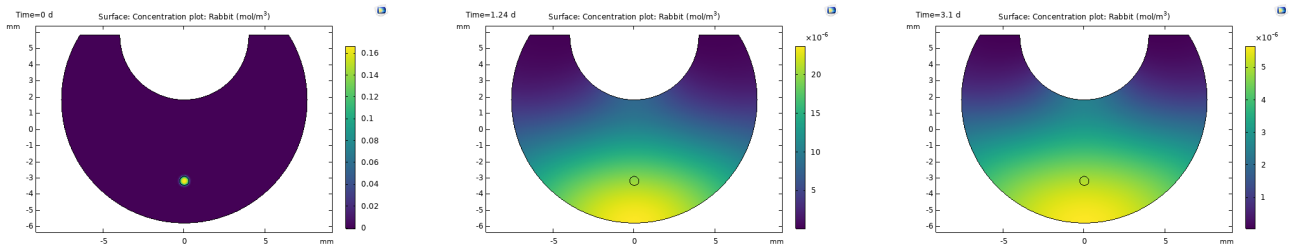

(a) $t = 0$ days (b) $t = 1.2$ days (c) $t = 3.1$ days

Figure 6: 2D plot of drug transport in vitreous, drug injected location (0,0,-5): rabbit

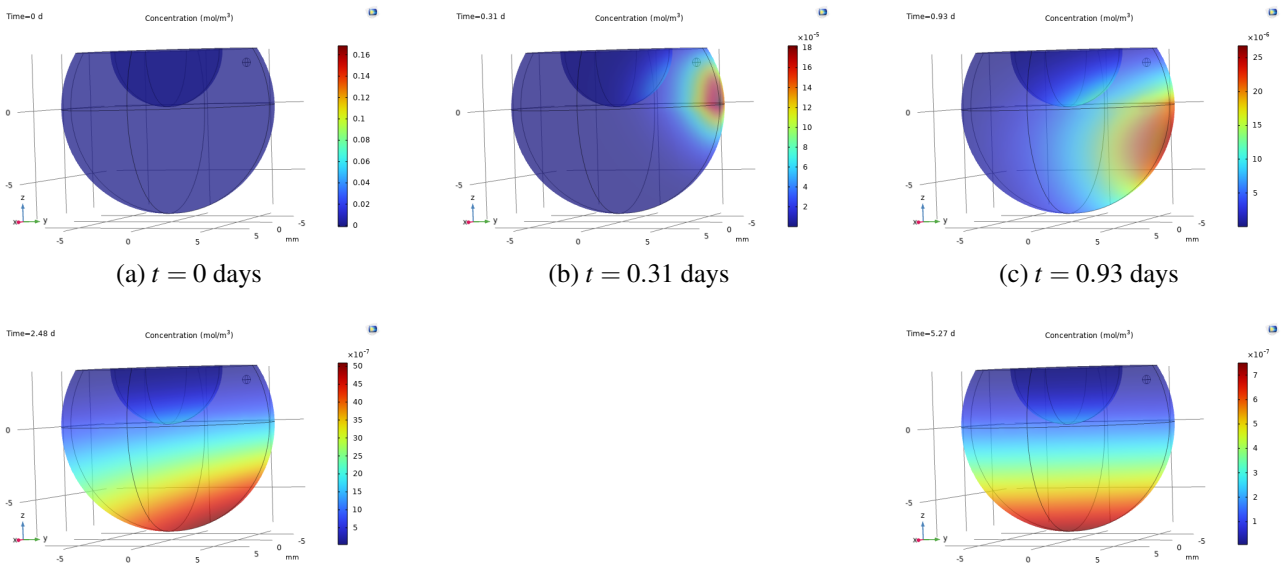

(a) $t = 0$ days (b) $t = 0.31$ days (c) $t = 0.93$ days

(d) $t = 2.48$ days (e) $t = 5.27$ days

Figure 7: 3D plot of drug transport in vitreous, drug injected location (0,6,3): rabbit

us to use the same value in the human model. In the experimental data [36], the maximum concentration of vitreous humor after administration was, C_{max} = 0.163 µg/mL where in our COMSOL model, the C_{max}= 0.6 µg/mL, which is close to the experimental value. Fig. 8 includes the concentration profiles in human vitreous taken from experimental study and results from our computational model. Our results are in good agreement with the experimental results obtained.

In the study by Beer et al. [37], the vitreous humor samples were taken at 48 hours and 4 weeks for measuring the drug concentration of bevacizumab for two patients. The drug was injected at the near limbus location in the posterior of the eye. For patient 1, the drug concentration was found 3.33×10^{-12} mol/mL at 4 weeks after the bevacizumab injection. In our computational model, the drug bevacizumab concentration was found 3.33×10^{-12} mol/mL within 2 weeks. For patient 2, the same amount of drug concentration in the vitreous was found within 48 hours. Both patients have different types of retinal disease and underlying surgical conditions. However, the fact that our results only focus on AMD condition that was different from those two conditions but using the same drug was the reason to compare those results in our study

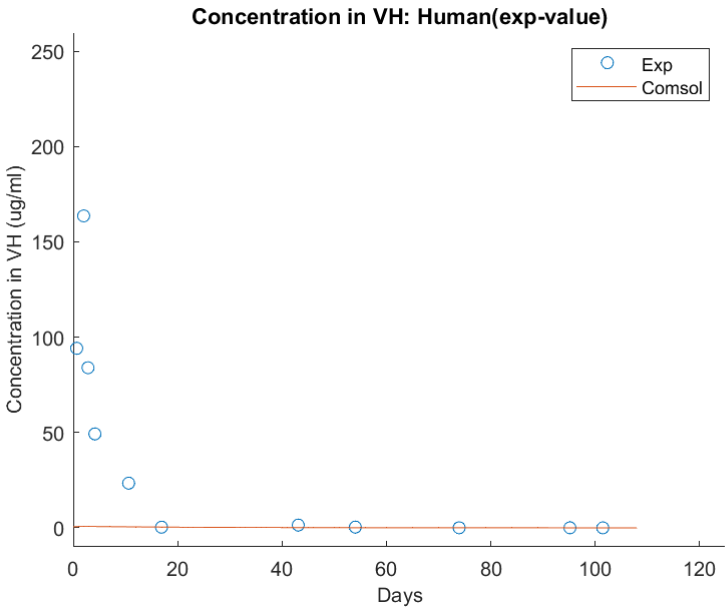

Figure 8: Drug concentration in VH: human

The major purpose of using the drug bevacizumab is to control VEGF in the macula region and the concentration near the macula includes in Fig. 9. While the drug is injected near the limbus region at coordinates of (0,6,4), the C_{max} value is 0.678 µg/mL, and when the drug is administrated in the middle of vitreous humor(0,0,-5), C_{max} value is 0.6400 µg/mL. The concentration goes lower than 500 ng/mL after 17 days while injected near the limbus (0,6,3) region and 5 days while injected near the macula (0,0,-5) region in the human eye accordingly.

Khoobyar et al. [17] also tried different locations to observe spatial drug distribution in the human eye using mathematical modeling. They calculated the pressure plot in the human eye considering the vitreous humor divided into two different regions liquefied and gel-type regions. They have used different permeability values using for gel type and liquefied region under Darcy's law to simulate vitreous humor. They calculated the pressure distribution throughout the vitreous and obtained maximum pressure is 0.05 kPa [17]. In our model, we used Darcy's law to solve the vitreous as a whole domain as a porous structure. In our model, the maximum pressure we measured in the human geometry is 0.09 kPa shown in Fig. 10.

Fig. 11 shows the 2D plot including the spatial distribution of drug bevacizumab transport through the vitreous while the drug is injected in the central vitreous (0.0,-5). Fig. 112 shows the drug transport in a 3D plot.

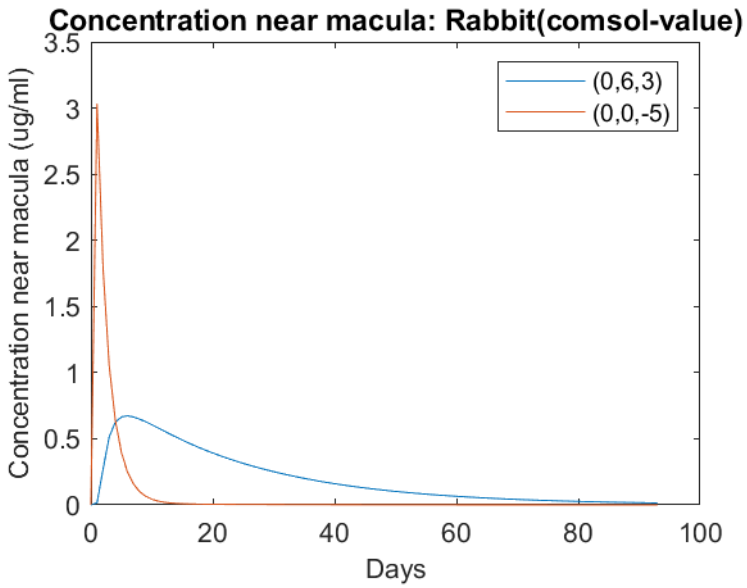

Figure 9: Drug concentration near macula: human

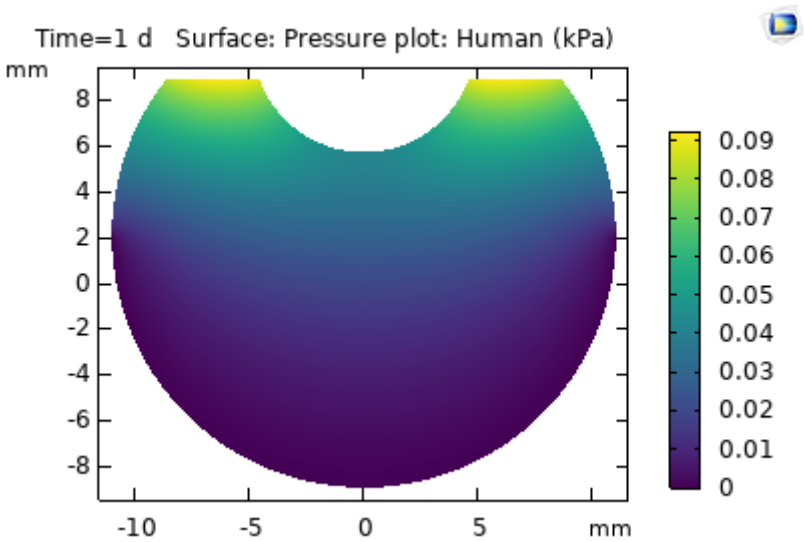

Figure 10: 2D pressure plot in human

3.3 Conclusions

Our pharmacokinetic model can provide a realistic estimate of bevacizumab transport in both human and rabbit eyes. The contribution of computationally implementing the drug concentration-time plot after intravitreal injection in the vitreous and near macula was validated with the experimentally published data. Both our models are in good agreement that the experimental results. The concentration near the macula also showed with the required amount of drug was present in that region that needed to reduce the vascular endothelial growth in the macula for AMD treatment. Our PK model successfully captures the drug absorption and distribution in the vitreous considering the elimination routes from published data. We can use our current PK model for future drug delivery systems using different drugs in AMD treatment to observe the drug kinetics. Our major goal of this work is to follow similar methods to solve the simulation in both geometries (human and rabbit) to prove that, our model can work in any animal model using the same methods.

Some limitations of the current work are that it focuses only on intravitreal injection. Others have considered modeling controlled-release drug delivery formulations for intravitreal delivery. Heljak and Swieszkowski [14] considered bevacizumab sustained release from drug-loaded microspheres.

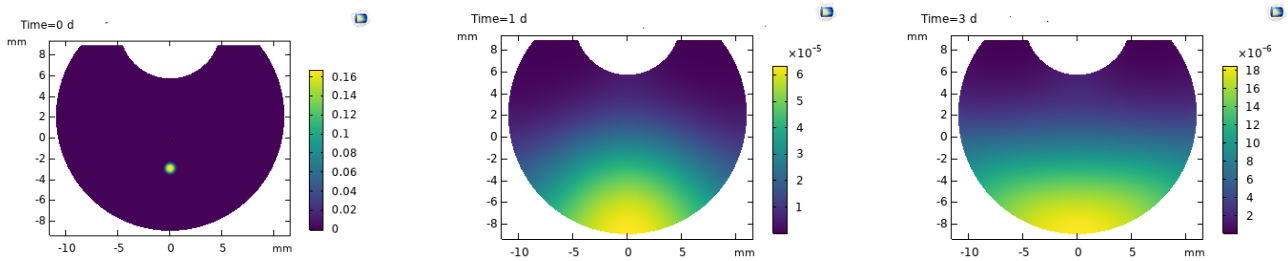

(a) $t = 0$ days (b) $t = 1$ days (c) $t = 3$ days

Figure 11: 2D plot of drug bevacizumab distribution in the human eye.

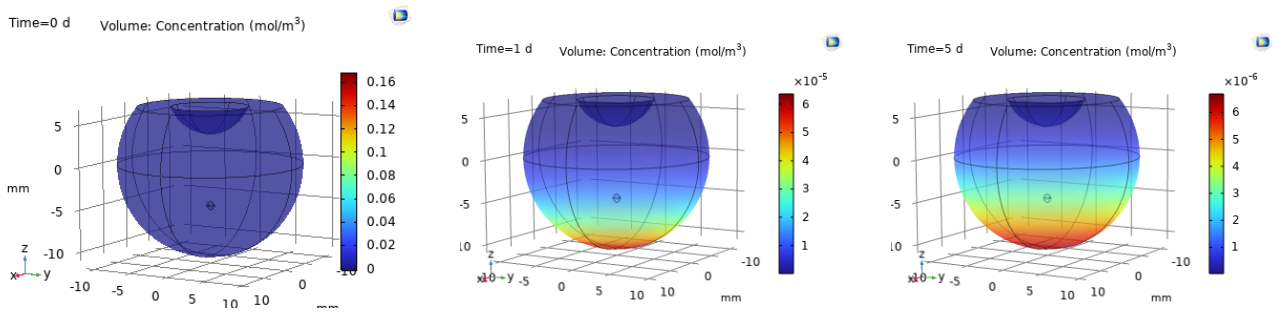

(a) $t = 0$ days (b) $t = 1$ days (c) $t = 5$ days

Figure 12: 3D plot of drug bevacizumab transport in vitreous, drug injected location(0,0,-5): human

Van Kampen et al. [38] considered a hollow hyaluronic acid cylinder intravitreally implanted in the vitreous to observe the drug bevacizumab release in retinal treatment; a major focus of the work was to model the drug diffusion coefficients of the implanted hollow cylinder, changing the size (inner and outer radius of the cylinder) so that it could hold the drug for four months. These are directions the current work could be extended towards.

The drug transport in the rabbit eye for the first few days is faster in our model than in other experimental studies. It diffuses faster than other experimental models. The physiological and material properties of the vitreous vary a little amount of scale and are not similar for every vitreous. As the drug transport depends on the physiological properties of vitreous humor so we have found various concentration profiles for different PK studies done experimentally. Using injection is one of the current treatment processes for AMD but patient faces frequent amount of injection as the drug was transported faster in this process. We are trying to implement drug-loaded micro-spheres so that drugs can present longer than this injection method in our future work.

3.4 Appendix

More results of rabbit eye are included in Fig. 13 and Fig. 14.

4 Acknowledgments

This work was supported by the National Institutes of Health grant R35GM133763 (ANFV).

References

[1] K. L. Pennington and M. M. DeAngelis. Epidemiology of age-related macular degeneration (AMD): associations with cardiovascular disease phenotypes and lipid factors. *Eye Vision*, 3:34,

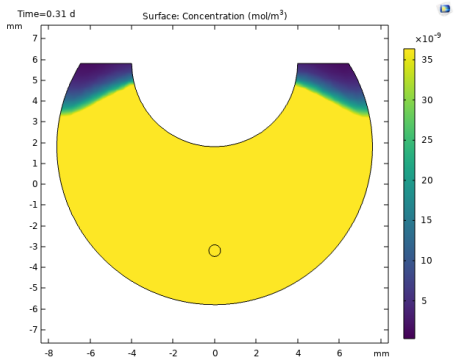

(a) $t = 0.3$ days

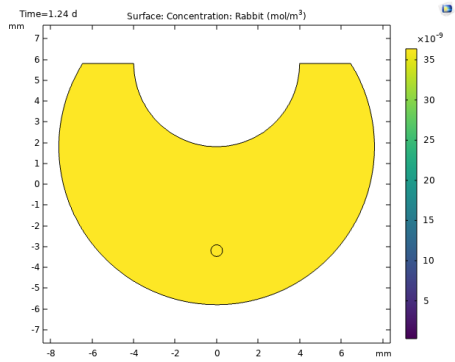

(b) $t = 1.2$ days

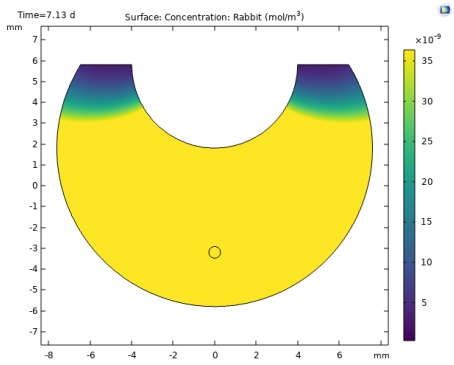

(c) $t = 7.13$ days

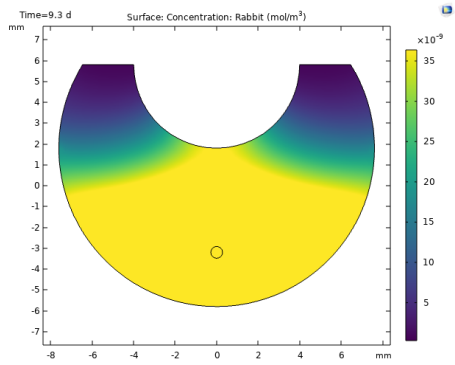

(d) $t = 9.3$ days

Figure 13: 2D plot of drug bevacizumab transport in the vitreous (0,0,-5): rabbit

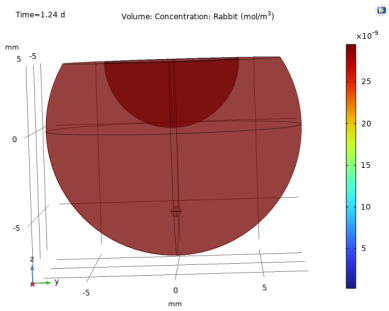

(a) $t = 0.24$ days

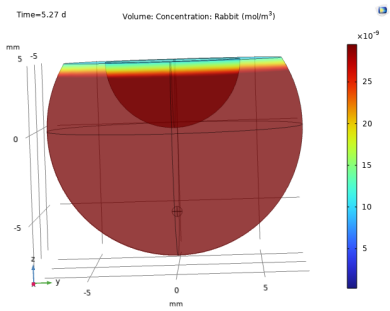

(b) $t = 5.27$ days

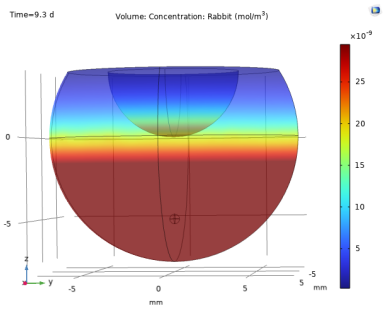

(c) $t = 9.3$ days

Figure 14: 3D plot of drug bevacizumab transport in the vitreous (0,0,-5): rabbit

2016.

[2] M. M. DeAngelis, L. A. Owen, M. A. Morrison, D. J. Morgan, M. Li, A. Shakoor, A. Vitale, S. Iyengar, D. Stambolian, I. K Kim, et al. Genetics of age-related macular degeneration (AMD). *Human Molecular Genetics*, 26(R1):R45–R50, 2017.

[3] M. Hadziahmetovic and G. Malek. Age-related macular degeneration revisited: From pathology and cellular stress to potential therapies. *Frontiers in Cell and Developmental Biology*, 8:612812, 2021.

[4] A. Stahl. The diagnosis and treatment of age-related macular degeneration. *Deutsches Ärzteblatt International*, 117(29-30):513, 2020.

[5] J. Mains and C. G Wilson. The vitreous humor as a barrier to nanoparticle distribution. *Journal of Ocular Pharmacology and Therapeutics*, 29(2):143–150, 2013.

[6] R. L. Zimmerman. In vivo measurements of the viscoelasticity of the human vitreous humor. *Biophysical Journal*, 29(3):539–544, 1980.

[7] N. K. Tram and K. E. Swindle-Reilly. Rheological properties and age-related changes of the human vitreous humor. *Frontiers in Bioengineering and Biotechnology*, 6:199, 2018.

[8] S. Yang, J. Zhao, and X. Sun. Resistance to anti-vegf therapy in neovascular age-related macular degeneration: a comprehensive review. *Drug Design, Development and Therapy*, 10:1857, 2016.

[9] R. Klein, T. Peto, A. Bird, and M. R. Vannewkirk. The epidemiology of age-related macular degeneration. *American Journal of Ophthalmology*, 137(3):486–495, 2004.

[10] R. Varela-Fernandez, V. Diaz-Tome, A. Luaces-Rodriguez, A. Conde-Penedo, X. Garcia-Otero, A. Luzardo-Alvarez, A. Fernandez-Ferreiro, and F. J. Otero-Espinar. Drug delivery to the posterior segment of the eye: biopharmaceutic and pharmacokinetic considerations. *Pharmaceutics*, 12(3):269, 2020.

[11] S. J. Bakri, M. R. Snyder, J. M. Reid, J. S. Pulido, and R. J. Singh. Pharmacokinetics of intravitreal bevacizumab (avastin). *Ophthalmology*, 114(5):855–859, 2007.

[12] E. M. Del Amo and A. Urtti. Rabbit as an animal model for intravitreal pharmacokinetics: Clinical predictability and quality of the published data. *Experimental Eye Research*, 137:111–124, 2015.

[13] J. Ahn, H. Kim, S. J. Woo, J. H. Park, S. Park, D. J. Hwang, and K. H. Park. Pharmacokinetics of intravitreally injected bevacizumab in vitrectomized eyes. *Journal of Ocular Pharmacology and Therapeutics*, 29(7):612–618, 2013.

[14] M. K. Heljak and W. Swieszkowski. In silico model of bevacizumab sustained release from intravitreal administrated PLGA drug-loaded microspheres. *Material Letters*, 307:131080, 2022.

[15] P. Causin and F. Malgaroli. Mathematical assessment of drug build-up in the posterior eye following transscleral delivery. *Journal of Mathematics in Industry*, 6:9, 2016.

[16] L. A. Hutton-Smith, E. A. Gaffney, H. M. Byrne, P. K. Maini, D. Schwab, and N. A. Mazer. A mechanistic model of the intravitreal pharmacokinetics of large molecules and the pharmacodynamic suppression of ocular vascular endothelial growth factor levels by ranibizumab in patients with neovascular age-related macular degeneration. *Molecular Pharmaceutics*, 13(9):2941–2950, 2016.

[17] A. Khoobyar, A. N. Penkova, M. S. Humayun, and S. S. Sadhal. Mathematical model of macromolecular drug transport in a partially liquefied vitreous humor. *Journal of Heat Transfer*, 144(3):031208, 2022.

[18] R. K. Balachandran and V. H. Barocas. Contribution of saccadic motion to intravitreal drug transport: Theoretical analysis. *Pharmaceutical Research*, 28(5):1049–1064, 2011.

[19] A. Khoobyar, A. Naghdloo, A. N. Penkova, M. S. Humayun, and S. S. Sadhal. Analytical and computational modeling of sustained-release drug implants in the vitreous humor. *Journal of Heat Transfer*, 143(10):101201, 2021.

[20] M. Lamminsalo, E. Taskinen, T. Karvinen, A. Subrizi, L. Murtomaki, A. Urtti, and V. P. Ranta. Extended pharmacokinetic model of the rabbit eye for intravitreal and intracameral injections of macromolecules: Quantitative analysis of anterior and posterior elimination pathways. *Pharmaceutical Research*, 35(8):153, 2018.

[21] P. J. Missel, M. Horner, and R. Muralikrishnan. Simulating dissolution of intravitreal triamcinolone acetonide suspensions in an anatomically accurate rabbit eye model. *Pharmaceutical Research*, 27(8):1530–1546, 2010.

[22] P. J. Missel. Simulating intravitreal injections in anatomically accurate models for rabbit, monkey, and human eyes. *Pharmaceutical Research*, 29(12):3251–3272, 2012.

[23] A. M. Azhdam, R. A. Goldberg, and S. Ugradar. In vivo measurement of the human vitreous chamber volume using computed tomography imaging of 100 eyes. *Translational Vision Science & Technology*, 9(1):2, 2020.

[24] E. Jooybar, M. J. Abdekhodaie, F. Farhadi, and Y. L. Cheng. Computational modeling of drug distribution in the posterior segment of the eye: Effects of device variables and positions. *Mathematical Biosciences*, 255:11–20, 2014.

[25] R. K. Balachandran. *Computational modeling of drug transport in the posterior eye*. University of Minnesota, 2010.

[26] N. Haghjou, M. J. Abdekhodaie, Y. L. Cheng, and M. Saadatmand. Computer modeling of drug distribution after intravitreal administration. *International Journal of Pharmacological and Pharmaceutical Sciences*, 5(5):194–204, 2011.

[27] A. F. Silva, M. A. Alves, and M. S. N. Oliveira. Rheological behaviour of vitreous humour. *Rheologica Acta*, 56:377–386, 2017.

[28] C. I Sinapis, J. G Routsias, A. I Sinapis, D. I Sinapis, G. D Agrogiannis, A. Pantopoulou, S. E Theocharis, S. Baltatzis, E. Patsouris, and D. Perrea. Pharmacokinetics of intravitreal bevacizumab (avastin®) in rabbits. *Clinical Ophthalmology*, 5:697, 2011.

[29] A. Hård and A. Hellström. On safety, pharmacokinetics and dosage of bevacizumab in rop treatment–a review. *Acta Paediatrica*, 100(12):1523–1527, 2011.

[30] S. Zhang, A. Penkova, M. S. Humayun, J. C. Martinez-Camarillo, A. C. Tadle, A. Galesic, M. E. Thompson, M. Pratt, A. Gonzales-Calle, and S. S. Sadhal. In vivo experimental and analytical studies for bevacizumab diffusion coefficient measurement in the rabbit vitreous humor. *Journal of Heat Transfer*, 143(3), 2021.

[31] R. Ankit. *'Web based tool to extract data from plots, images, and maps'*, Version 4.6 Released (September 16, 2022). urlhttps://automeris.io/WebPlotDigitizer/.

[32] Z. Ye, Y. Ji, X. Ma, J. Wen, W. Wei, and S. Huang. Pharmacokinetics and distributions of bevacizumab by intravitreal injection of bevacizumab-plga microspheres in rabbits. *International Journal of Ophthalmology*, 8(4):653, 2015.

[33] R. Varshochian, M. Riazi-Esfahani, M. Jeddi-Tehrani, A. Mahmoudi, S. Aghazadeh, M. Mahbod, M. Movassat, F. Atyabi, A. Sabzevari, and R. Dinarvand. Albuminated PLGA nanoparticles containing bevacizumab intended for ocular neovascularization treatment. *Journal of Biomedical Materials Research, Part A*, 103(10):3148–3156, 2015.

[34] H. Nomoto, F. Shiraga, N. Kuno, E. Kimura, S. Fujii, K. Shinomiya, A. K Nugent, K. Hirooka, and T. Baba. Pharmacokinetics of bevacizumab after topical, subconjunctival, and intravitreal administration in rabbits. *Investigative Ophthalmology & Visual Science*, 50(10):4807–4813, 2009.

[35] S. Friedrich, Y. Cheng, and B. Saville. Finite element modeling of drug distribution in the vitreous humor of the rabbit eye. *Annals of Biomedical Engineering*, 25(2):303, 1997.

[36] Q. Zhu, F. Ziemssen, S. Henke-Fahle, O. Tatar, P. Szurman, S. Aisenbrey, N. Schneiderhan-Marra, X. Xu, S. Grisanti, Tübingen Bevacizumab Study Group, et al. Vitreous levels of bevacizumab and vascular endothelial growth factor-a in patients with choroidal neovascularization. *Ophthalmology*, 115(10):1750–1755, 2008.

[37] P. M. Beer, S. J. Wong, A. M. Hammad, N. S. Falk, M R. O'Malley, and S. Khan. Vitreous levels of unbound bevacizumab and unbound vascular endothelial growth factor in two patients. *Retina*, 26(8):871–876, 2006.

[38] E. Van Kampen, C. Vandervelden, A. Fakhari, J. Qian, C. Berkland, and S. H. Gehrke. Design of hollow hyaluronic acid cylinders for sustained intravitreal protein delivery. *Journal of Pharmaceutical Sciences*, 107(9):2354–2365, 2018.